

Large-size, high-uniformity, random silver nanowire networks as transparent electrodes for crystalline silicon wafer solar cells

Shouyi Xie, Zi Ouyang, Baohua Jia, and Min Gu*

Centre for Micro-Photonics, Faculty of Engineering and Industrial Sciences, Swinburne University of Technology,
P.O. Box 218, Hawthorn, 3122 Victoria, Australia

*mgu@swin.edu.au

Abstract: Metal nanowire networks are emerging as next generation transparent electrodes for photovoltaic devices. We demonstrate the application of random silver nanowire networks as the top electrode on crystalline silicon wafer solar cells. The dependence of transmittance and sheet resistance on the surface coverage is measured. Superior optical and electrical properties are observed due to the large-size, highly-uniform nature of these networks. When applying the nanowire networks on the solar cells with an optimized two-step annealing process, we achieved as large as 19% enhancement on the energy conversion efficiency. The detailed analysis reveals that the enhancement is mainly caused by the improved electrical properties of the solar cells due to the silver nanowire networks. Our result reveals that this technology is a promising alternative transparent electrode technology for crystalline silicon wafer solar cells.

©2013 Optical Society of America

OCIS codes: (160.2100) Electro-optical materials; (160.6000) Semiconductor materials; (230.2090) Electro-optical devices.

References and links

1. A. Luque and S. Hegedus, *Handbook of Photovoltaic Science and Engineering* (Wiley, 2010).
2. M. A. Green, *Third Generation Photovoltaics: Advanced Solar Energy Conversion* (Springer, 2003).
3. H. A. Atwater and A. Polman, "Plasmonics for improved photovoltaic devices," *Nat. Mater.* **9**(3), 205–213 (2010).
4. M. Gu, Z. Ouyang, B. Jia, N. Stokes, X. Chen, N. Fahim, X. Li, M. J. Ventura, and Z. Shi, "Nanoplasmonics: a frontier of photovoltaic solar cells," *Nanophotonics* **1**(3-4), 235–248 (2012).
5. X. Chen, B. Jia, J. K. Saha, B. Cai, N. Stokes, Q. Qiao, Y. Wang, Z. Shi, and M. Gu, "Broadband enhancement in thin-film amorphous silicon solar cells enabled by nucleated silver nanoparticles," *Nano Lett.* **12**(5), 2187–2192 (2012).
6. Z. Ouyang, S. Pillai, F. Beck, O. Kunz, S. Varlamov, K. R. Catchpole, P. Campbell, and M. A. Green, "Effective light trapping in polycrystalline silicon thin-film solar cells by means of rear localized surface plasmons," *Appl. Phys. Lett.* **96**(26), 261109 (2010).
7. N. F. Fahim, B. Jia, Z. Shi, and M. Gu, "Simultaneous broadband light trapping and fill factor enhancement in crystalline silicon solar cells induced by Ag nanoparticles and nanoshells," *Opt. Express* **20**(S5 Suppl 5), A694–A705 (2012).
8. A. Shalav, B. S. Richards, and M. A. Green, "Luminescent layers for enhanced silicon solar cell performance: Up-conversion," *Sol. Energy Mater. Sol. Cells* **91**(9), 829–842 (2007).
9. D. S. Hecht, L. Hu, and G. Irvin, "Emerging transparent electrodes based on thin films of carbon nanotubes, graphene, and metallic nanostructures," *Adv. Mater.* **23**(13), 1482–1513 (2011).
10. L. Hu, H. S. Kim, J.-Y. Lee, P. Peumans, and Y. Cui, "Scalable coating and properties of transparent, flexible, silver nanowire electrodes," *ACS Nano* **4**(5), 2955–2963 (2010).
11. A. Sugianto, O. Breitenstein, B. S. Tjahjono, A. Lennon, L. Mai, and S. R. Wenham, "Impact of localized regions with very high series resistances on cell performance," *Prog. Photovolt. Res. Appl.* **20**(4), 452–462 (2012).
12. J.-Y. Lee, S. T. Connor, Y. Cui, and P. Peumans, "Solution-processed metal nanowire mesh transparent electrodes," *Nano Lett.* **8**(2), 689–692 (2008).
13. J.-Y. Lee, S. T. Connor, Y. Cui, and P. Peumans, "Semitransparent organic photovoltaic cells with laminated top electrode," *Nano Lett.* **10**(4), 1276–1279 (2010).
14. C.-H. Liu and X. Yu, "Silver nanowire-based transparent, flexible, and conductive thin film," *Nanoscale Res. Lett.* **6**(1), 75 (2011).

15. V. Scardaci, R. Coull, P. E. Lyons, D. Rickard, and J. N. Coleman, "Spray deposition of highly transparent, low-resistance networks of silver nanowires over large areas," *Small* **7**(18), 2621–2628 (2011).
16. A. R. Madaria, A. Kumar, F. N. Ishikawa, and C. Zhou, "Uniform, highly conductive, and patterned transparent films of a percolating silver nanowire network on rigid and flexible substrates using a dry transfer technique," *Nano Res.* **3**(8), 564–573 (2010).
17. M. G. Kang and L. J. Guo, "Nanoimprinted semitransparent metal electrodes and their application in organic light-emitting diodes," *Adv. Mater.* **19**(10), 1391–1396 (2007).
18. L. J. Guo, "Nanoimprint lithography: methods and material requirements," *Adv. Mater.* **19**(4), 495–513 (2007).
19. Solarbuzz, "Solar market research and analysis" (2012), retrieved <http://www.solarbuzz.com/going-solar/understanding/technologies>.
20. W. Gaynor, J.-Y. Lee, and P. Peumans, "Fully solution-processed inverted polymer solar cells with laminated nanowire electrodes," *ACS Nano* **4**(1), 30–34 (2010).
21. M.-G. Kang, M.-S. Kim, J. Kim, and L. J. Guo, "Organic solar cells using nanoimprinted transparent metal electrode," *Adv. Mater.* **20**, 6 (2008).
22. B. E. Hardin, W. Gaynor, I. K. Ding, S.-B. Rim, P. Peumans, and M. D. McGehee, "Laminating solution-processed silver nanowire mesh electrodes onto solid-state dye-sensitized solar cells," *Org. Electron.* **12**(6), 875–879 (2011).
23. L. E. Scriven, "Physics and applications of dip coating and spin coating," *MRS Online Proc. Library* **121** (1988).
24. T. M. Barnes, M. O. Reese, J. D. Bergeson, B. A. Larsen, J. L. Blackburn, M. C. Beard, J. Bult, and J. van de Lagemaat, "Comparing the fundamental physics and device performance of transparent, conductive nanostructured networks with conventional transparent conducting oxides," *Adv. Energy Mater.* **2**(3), 353–360 (2012).
25. Y. Zhang, Z. Ouyang, N. Stokes, B. Jia, Z. Shi, and M. Gu, "Low cost and high performance Al nanoparticles for broadband light trapping in Si wafer solar cells," *Appl. Phys. Lett.* **100**(15), 151101 (2012).
26. W. Shockley and H. J. Queisser, "Detailed balance limit of efficiency of p-n junction solar cells," *J. Appl. Phys.* **32**(3), 510–519 (1961).
27. K. L. Chopra, S. Major, and D. K. Pandya, "Transparent conductors—A status review," *Thin Solid Films* **102**(1), 1–46 (1983).
28. D. Stauffer and A. Aharony, *Introduction To Percolation Theory*, 2nd ed. (Taylor & Francis, 1994).
29. P. Heitjans and J. Kärger, *Diffusion in Condensed Matter: Methods, Materials, Models* (Springer-Verlag Berlin Heidelberg, 2005), Vol. 22.
30. A. M. Cowley and S. M. Sze, "Surface states and barrier height of metal-semiconductor systems," *J. Appl. Phys.* **36**(10), 3212–3220 (1965).
31. D. A. Clugston and P. A. Basore, "PC1D version 5: 32-bit solar cell modeling on personal computers," in *Record of 26th IEEE Photovoltaic Specialists Conference*, (Institute of Electrical and Electronics Engineers, 1997), pp. 207–210.

1. Introduction

Numerous "next generation" photovoltaic solar cells based on nanostructure engineering have been proposed to improve the energy conversion efficiencies and reduce the costs [1–9]. Most of these nanostructures are designed to improve one aspect within the photovoltaic process, which in principle involves (i) absorption of photons [3–7], (ii) energy transfer from photons to electrons [8] and (iii) transport of the charges out of the devices by the electrodes [9]. Among all the proposed approaches, using metal nanowire (NW) networks to replace the conventional top electrodes is of particular interest, as the top electrodes fundamentally link to both the optical aspect and the electrical aspect of a photovoltaic device. Therefore, any improved designs on the top electrode tend to result in large performance improvements. For an electrode on top of a solar cell in general, the most important design principle is to achieve a high transmittance while keeping the conductance high, which are essentially two opposing factors. Encouragingly, the metal NW networks have shown a great potential to replace conventional transparent conductive oxides (TCOs), as the former has been found to be superior in terms of conductance and transmittance performance [10].

Although the metal NW electrodes show promises, there lie three major challenges: (i) the networks have not been demonstrated to be uniform over a solar cell scale at affordable expenses, which is a bottleneck for the photovoltaic application of this technology. A full-sized solar cell can be considered as numerous "sub-sized" solar cells connected in parallel. If high series resistance presents on some of the "sub-sized" solar cells, the electricity output of the good "sub-sized" cells can be compensated and the overall performance of the cell can be severely affected by these "bad spots" [11]. However, the reported methods for NW network fabrication, such as drop-casting [12,13], Meyer-rod-coating [10,14], spray-coating [15] and dry transferring [16], have not shown uniform NW networks over a large area, which

essentially limits the application to large-size solar cells. On the other hand, although lithography-based methods can produce large-scale, uniform NW networks in principle [17,18], volume production is challenging due to the high costs. (ii) Better optical and electrical performance of the NW electrodes is needed in order to maximize the potential of metal NW electrodes as a replacement of conventional top electrodes. It means that the optical loss due to reflectance and parasitic absorption in the electrodes has to be reduced and in the meantime, the resistive loss in the metal NWs has to be reduced. (iii) Finally, this technology has not yet been demonstrated on inorganic, particularly silicon-based solar cells that dominate the photovoltaic market with a share of more than 80% [19]. Most of the reported work is the NW electrodes for organic-based solar cells [20–22].

To address the above-mentioned challenges, this paper demonstrates a spin-coating based fabrication method for large-size, high-uniformity, random AgNW electrodes for the crystalline silicon wafer solar cells. The transmittance and sheet resistance of the AgNW networks are first characterized on glass substrates. The coating conditions and the post-deposition annealing conditions are investigated to optimize the optical and electrical performance of the AgNW networks. The optimized AgNW networks are then integrated on crystalline silicon wafer solar cells. Surface morphology, series resistance, external quantum efficiency and I - V characteristics of the solar cells are characterized in order to determine the performance of the AgNW electrodes. With an optimized two-step annealing process, a significant performance enhancement up to 19% is observed with the NW electrodes.

2. Optical and electrical properties of the AgNW networks

Prior to depositing the AgNWs on silicon wafer solar cells, we first fabricated them on the glass substrates for investigating and optimizing the optical and electrical performance of the AgNWs. This effect is necessary because the silicon wafers are optically absorbing and electrically conductive, which can disturb the correct interpretation of the properties of AgNWs. The glass slides were firstly coated with poly-*l*-lysine to increase the affinity of the AgNWs to the glass [13]. Concentrated AgNW suspension (from Seashell Technology, average NW diameter of 100 nm and NW length of 30 μ m) in isopropyl alcohol was diluted by about one-thousand times. The suspension was then deposited onto the glass substrates by spin-coating at a rotary speed of 800 rpm, as schematically shown in Fig. 1(a). With controlled suspension volume, surface preparation and spinning conditions, the AgNWs could uniformly cover the entire 2.5 cm \times 2.5 cm glass slides with a tunable surface coverage (SC) from 10% to 40%. The superior geometrical uniformity, with a SC variation of less than \pm 3% over the entire surface of one sample, was confirmed by a large number of scanning electron microscope (SEM) images (totally 0.5 mm² for each sample). One typical SEM image is shown in Fig. 1(b). The uniformity of the electrical conductance, with a variation of less than \pm 10% over one sample, was confirmed via the four-point-probe sheet resistance (R_{sh}) measurements at five random spots on each sample. Such a high level of the uniformity has not been observed on NW networks fabricated via other methods, such as drop-casting [13], meyer-rod coating [10,14], spray coating [15] and dry transferring [16], which have a typical SC variation of about 10% [15], or R_{sh} variation of about 55% [16]. We believe that the competition between the centrifugal force and the viscous force of the liquid in the spin-coating process, which does not exist in other deposition methods, helps the uniform deposition of the nanostructure networks [23]. As a result, our method does not suffer from the severe agglomeration or non-uniform distribution of NWs.

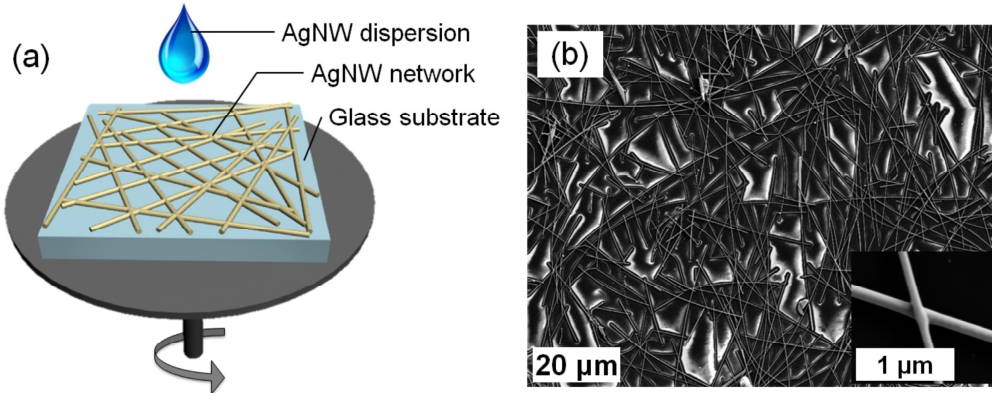


Fig. 1. (a) Schematic diagram of spin-coating a AgNW network on a glass substrate. (b) An SEM image of the spin-coated AgNW network. Inset: a fused junction between two AgNWs after annealing at 200 °C for 30 min.

After the AgNW coating process, a following low-temperature annealing process was performed (N_2 atmosphere at 200 °C for 30 min) in order to evaporate the residual surfactant and fuse the junction points of NW connections, as shown in the inset of Fig. 1(b). The conductance of the networks could improve as much as 80% after the optimized annealing process. The transmittance (T) of the AgNW networks was measured by spectrometry with an integrating sphere. Figure 2(a) shows the measured transmittance with variable R_{sh} of the AgNW networks, normalized to the transmittance of the bare glass substrate. R_{sh} was controlled by different AgNW SCs on the glass surface. A broadband high transmittance for wavelengths longer than 400 nm is observed for the AgNWs, while for an 80-nm thick, commercial-grade TCO film (from Suntech Power Holdings Co., Ltd.) the transmittance beyond 900 nm is severely decreased due to the free-carrier absorption in the film [24]. The narrow dips of the AgNW transmittance at ~ 350 nm are due to the localized surface plasmon resonance.

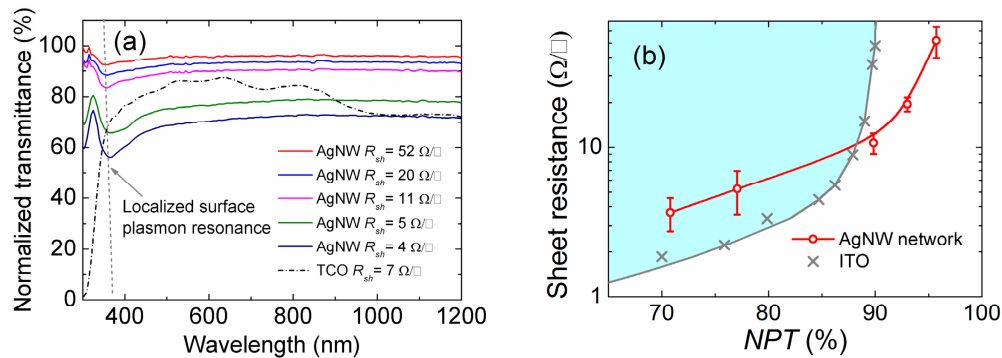


Fig. 2. (a) Measured transmittance with variable sheet resistance (R_{sh}) of AgNW networks (solid lines), normalized to the transmittance of the bare glass substrate. The measured data for a commercial-grade TCO film (dashed line) is presented as a reference. (b) Number of photons transmitted (NPT) as a function of R_{sh} for the AgNW networks (red circles). The data for ITO (gray crosses) is presented as a reference [27]. The AgNW networks in the white area can outperform the ITO.

We use a figure of merit, the number of photons transmitted (NPT), to evaluate the optical and electrical performance of the AgNW networks, as shown in Fig. 2(b). The NPT is defined as integrated transmittance over a wavelength range, where air mass 1.5 spectrum global (AM1.5G) is assigned as a weight factor for each wavelength [25]. The NPT determines the maximum available solar spectrum after passing the AgNW network that can be absorbed by

the solar cell and eventually links to the maximum photocurrent that the solar cell can possibly produce under the Shockley-Queisser limit [26]. The wavelength range was set to 400 – 900 nm in this work, representing the most important region for all types of solar cells in general. Figure 2(b) shows that the AgNW networks outperform the indium tin oxide (ITO) [27], a widely-used TCO electrode, once the *NPT* is larger than ~90%. Compared with other state-of-the-art AgNW networks in literature [10], the AgNW networks produced in this work outperform the *NPT* as much as 10% under the same sheet resistance conditions, or vice versa.

We attribute the outstanding performance to the aggregation-free, high-uniformity nature of the AgNW networks. With an optimized deposition and annealing control process, we can minimize the dangling NWs in a network. The absence of dangling NWs is beneficial for three reasons: (i) the dangling NWs can hardly contribute to the electron transportation. They have small-area point contacts (instead of large-area line contacts) to the silicon, which limits their capability to extract the electrons out of the active layer. Additionally, a dangling NW has a reduced chance to contact with other NWs in a network, making the network less conductive. (ii) According to the percolation theory, which is a standard physics model for describing a random network [16,28,29], a three-dimensional percolation network (aggregated networks containing the dangling NWs) has a larger dimensional factor compared with a two-dimensional network (free of the dangling NWs), which directly results in poorer conductance under the same *SC* conditions. (iii) While the dangling NWs do not contribute to electron conduction, they still reduce the *NPT* due to the parasitic absorption and reflection of the light. Compared with most of the published AgNW networks which suffer from aggregated clusters [14,15], our aggregation-free, high-uniformity networks have advantages in their application to solar cells in terms of the optical and electrical properties.

3. AgNW networks for crystalline silicon solar cells

Having the AgNW networks with excellent optical and electrical performance obtained, we carried out the proof-of-concept experiments of integrating the AgNW networks on crystalline silicon wafer solar cells for the first time. Figure 3(a) shows the structure of the cells. Aluminum rear contacts and front collection pads were deposited on two terminals of the *p*-type emitter/*n*-type base wafers (2 cm × 2 cm × 180 μm) for probe contact during the electrical measurements. The native oxide layer was removed by hydrofluoric acid prior to the spin-coating process of the AgNW dispersion on the front surface of the solar cell, ensuring the contact between the NWs and the silicon. Important parameters of solar cells, such as the series resistance (R_s), the external quantum efficiency (*EQE*), the short-circuit current density (J_{SC}), the open-circuit voltage (V_{OC}), the fill factor (*FF*) and the efficiency (η) were measured at each step of the fabrication process. Reference cells without the AgNWs were used alongside to exclude the experimental effects other than the AgNWs.

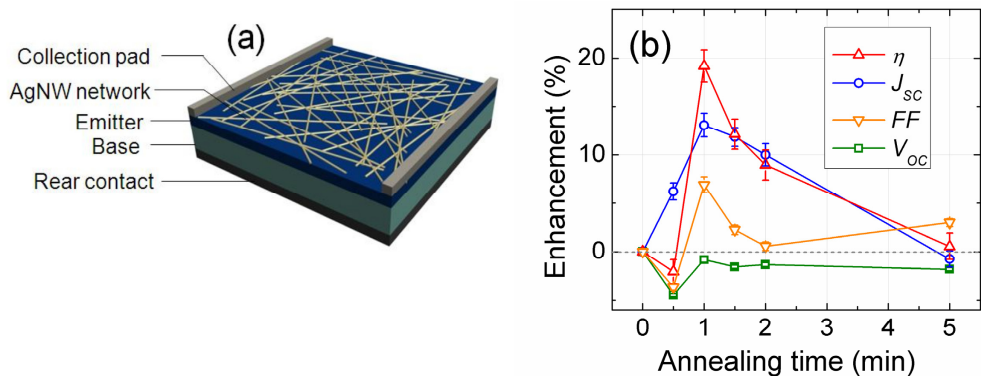


Fig. 3. (a) Schematic structure of a crystalline silicon wafer solar cell with a AgNW network as an electrode. (b) Enhancement of efficiency (η), short-circuit current (J_{sc}), fill factor (FF) and open-circuit voltage (V_{oc}) of the solar cells as a function of the annealing time at 400 °C.

As previously investigated on the glass substrates, the AgNW networks reach the maximum conductance after being annealed at 200 °C for 30 min due to the removal of the residual surfactant and fusion of the AgNW junctions. However, the solar cell performance did not improve after the low-temperature annealing process. We attribute to the fact that 200 °C is not high enough to form good ohmic contact between the AgNW networks and the silicon. Although the AgNW and silicon are physically in touch, a potential barrier of the Fermi level can exist on the AgNW/silicon interface [30], and thus the electrons in the silicon cannot freely travel through the interface to the NWs. It means that the electrons cannot be effectively extracted from the silicon to the AgNWs, even though the electrons can easily transport in the network due to the low network resistance. Therefore, another critical high-temperature annealing process at 400 °C for up to 5 min in the N₂ atmosphere was performed. The solar cell performance as a function of the high-temperature annealing time is shown in Fig. 3(b). It is noted that the optical and electrical properties of the NWs was unchanged within eighteen months. Hence under normal solar cell operating conditions, degradation of the NW performance is not expected. A significant efficiency enhancement of 19% (from 4.47% to 5.32%) was observed at 1 min. When the annealing time was prolonged to 5 min, the efficiency drops back close to the initial value. During the annealing process the variation of the V_{oc} value was negligible, indicating that the surface passivation was not affected by the metal-semiconductor interfacial states. Additionally, the figure clearly shows that the variation of the efficiency is mainly affected by J_{sc} .

The increase of the J_{sc} value may be due to (i) a larger quantity of generated electrons (light absorption) or (ii) a larger quantity of collected electrons. We attribute the J_{sc} enhancement mainly to reason (ii), the improved electron collection due to the AgNW electrode. Without the AgNWs contacting with the silicon, the electrons otherwise have to travel far in the silicon before they are collected by the pads. Therefore the chances for them to recombine or lose their momentum would be larger. This mechanism is confirmed in Fig. 4, where the series resistance (R_s) of the solar cells as a function of the high-temperature annealing time is presented, along with the SEM images of the NW conditions at each time spot. It is found that the R_s value first decreased by 26% at 1 min, and then increased gradually. This trend matches exactly with that of J_{sc} , the FF and the efficiency change. This observation is also in line with the condition change of the NWs indicated in the SEM images: from 2 min onwards, the NWs started to turn thinner, then break, and finally became isolated at 5 min. As a result, the optimum annealing time is 1 min, where a good AgNW/silicon contact condition is formed, and the quality of the AgNW networks is not yet compromised. At 5 min, the isolated silver particles can still provide the low-resistance bypass routes for the electrons at local spots, but the benefits to R_s and then the efficiency are limited.

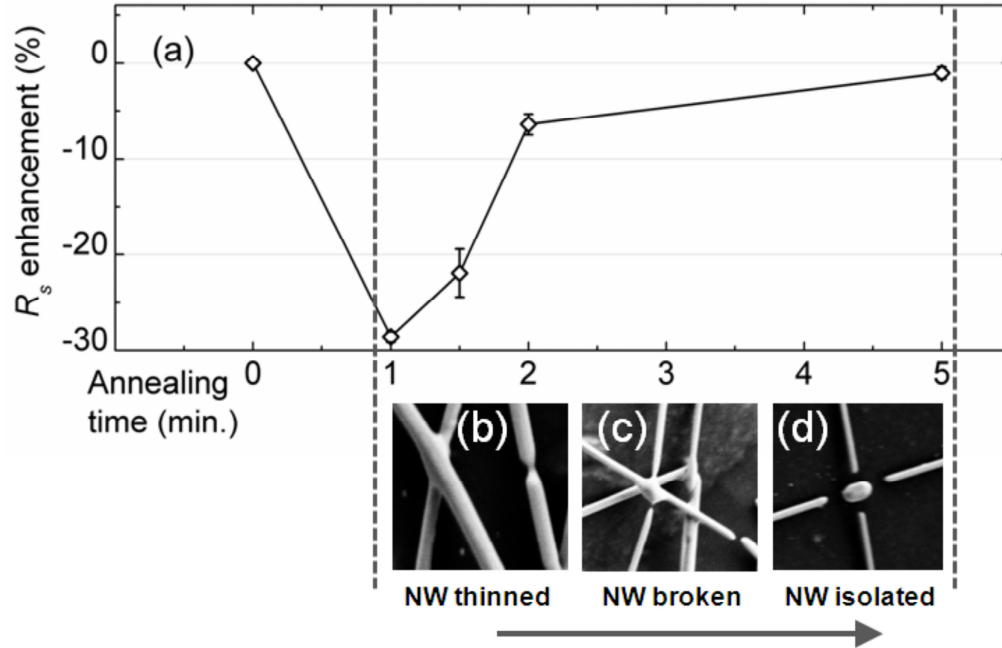


Fig. 4. (a) Series resistance (R_s) enhancement of the solar cells as a function of the annealing time at 400 °C. (b) – (d) evolution of the AgNW conditions by the annealing time.

We then performed *EQE* measurements to investigate if there is a significant change of light absorption, which can also affect J_{SC} of the solar cells. *EQE* is defined as the number of the generated electrons over the number of the illuminated photons and thus directly links to the light absorption in the silicon active layer, which is fundamentally more accurate over spectroscopy reflectance measurements that cannot exclude the parasitic absorption of photons in the metal NWs. The experiments were conducted at low light intensity and zero voltage bias, ensuring the solar cell resistance has negligible effects on the electron generation rate. The measurements show that there is 3.1% less photons absorbed by the silicon after the AgNW networks is applied. Two optical behaviors of AgNWs on silicon are responsible for this phenomenon. In the shorter wavelength range of 300 – 400 nm, light absorption in silicon can be reduced by the absorption peak in the AgNWs due to the surface plasmon resonance around 350 nm, as indicated in Fig. 2(a). In the longer wavelength range of 600 – 1200 nm, the use of AgNWs slightly increases the reflection. According to the integrated *EQE* over the AM1.5G spectrum, a 3.1% loss of number of photons can result in a relative efficiency loss of 0.3%, providing that the other parameters are considered unchanged. This is a negligible loss compared with a 19% efficiency enhancement determined by the *I-V* characterization, indicating that the much improved electron collection due to the AgNW networks is the main reason behind the efficiency enhancement.

Furthermore, the measured emitter R_{sh} and other parameters were input in a photovoltaic device simulation program PC1D [31]. Taken the optical loss factor and the electrical gain factor of the AgNW networks into account, the efficiency of the solar cell should increase from 4.47% to 5.69% with a relative enhancement of 27%, other than the measured enhancement of 19%. We attribute the discrepancy to the fact that after annealing at 400 °C for 1 min, the contact resistance between the AgNWs and the silicon still exists, although the network itself is already highly conductive. This hypothesis was confirmed by the fact that a perfect match between the characterization and simulation was achieved if a contact resistance of 0.3 Ω was inserted in the simulation model.

4. Conclusions

In conclusion, we have fabricated spin-coating based, large-size, high-uniformity, random silver NW networks as transparent electrodes for the crystalline silicon solar cells. The networks have been demonstrated to be highly uniform. The optical and electrical performance of the silver nanowire networks is superior to ITO and other types of silver nanowire meshes. Over 95% transmittance can be achieved for sheet resistance of $52 \Omega/\square$, and 93% transmittance for sheet resistance of as low as $30 \Omega/\square$. After an optimized critical two-step annealing process, a 19% enhancement on the solar cell energy conversion efficiency can be achieved as a result of the reduced series resistance and increased photocurrent. Larger enhancement is expected with improved contact between the nanowires and the silicon on a better fabrication process. Therefore, the silver nanowire networks are a promising alternative transparent electrode technology for crystalline silicon solar cells and other photovoltaic devices, due to the superior optical and electrical performance, processing simplicity and low costs.

Acknowledgments

The authors acknowledge the technical support from the Victoria-Suntech Advanced Solar Facility established under the Victoria Science Agenda of the Victorian Government. S.X. thanks Swinburne University of Technology for the SUPRA scholarship. B.J. thanks the Victorian Government for the support through the Victorian Fellowship. Boyuan Cai provided his assistance in the measurement data for the TCO in Fig. 2(a).